B

Simulation of Regional Climate Change with Global Coupled Climate Models and Regional Modeling Techniques

This Annex is based solely on Chapter 6 of the Working Group I contribution to the IPCC Second Assessment Report (1996).

F. GIORGI (USA), G.A. MEEHL (USA), A. KATTENBERG (THE NETHERLANDS), H. GRASSL (SWITZERLAND), J.F.B. MITCHELL (UK), R.J. STOUFFER (USA), T. TOKIOKA (JAPAN), A.J. WEAVER (CANADA), AND T.M.L. WIGLEY (USA)

CONTENTS

In IPCC (1990) and IPCC (1992), very low confidence was placed on the climate change scenarios produced by general circulation model (GCM) equilibrium experiments on the subcontinental, or regional, scale (order of 10^5–10^7 km^2). This was mainly attributed to coarse model resolution, limitations in model physics representations, errors in model simulation of present-day regional climate features, and wide inter-model range of simulated regional change scenarios. Since then, transient runs with Atmosphere-Ocean GCMs (AOGCMs) have become available that allow a similar regional analysis. In addition, different regionalization techniques have been developed and tested in recent years to improve the simulation of regional climate change. This section examines regional change scenarios produced by new coupled GCM runs. Following the 1990 and 1992 reports, emphasis is placed on the simulation of seasonally averaged surface air temperature and precipitation, although the importance of higher order statistics and other surface climate variables for impact assessment is recognized (Kittel *et al.*, 1995; Mearns *et al.*, 1995a,b).

B.1. Regional Simulations by GCMs

In IPCC (1990), five regions were identified for analysis of regional climate change simulation: Central North America (CNA; 35-50°N, 85-105°W), South East Asia (SEA; 5-30°N, 70-105°E), Sahel (Africa) (SAH; 10-20°N, 20°W-40°E), Southern Europe (SEU; 35-50°N, 10 W- 45°E), and Australia (AUS; 12-45°S, 110-155°E). Output from different coupled model runs with dynamical oceans for these regions was analyzed by Cubash *et al*. (1994a), Whetton *et al*. (1996), and Kittel *et al*. (1997), while analysis over the Australian region from equilibrium simulations with mixed-layer ocean models was performed by Whetton *et al*. (1994). Results over two additional regions were analyzed by Raisanen (1995) for Northern Europe (NEU; land areas north of 50°N and west of 60°E) and Li *et al*. (1994) for East Asia (EAS; 15-60°N, 70-140°E). To summarize the findings of these works, Figure B-1 shows differences between region-average values at the time of CO_2 doubling and for the control run, and differences between control run averages and observations (hereafter referred to as bias), for winter and summer surface air temperature and precipitation. Note that these models contain increases of CO_2 only. Experiments including increased CO_2 and the effects of sulfate aerosols will be discussed later.

The biases are presented as a reference for the interpretation of the scenarios, because it can be generally expected that the better the match between control run and observed climate (i.e., the lower the biases), the higher the confidence in simulated

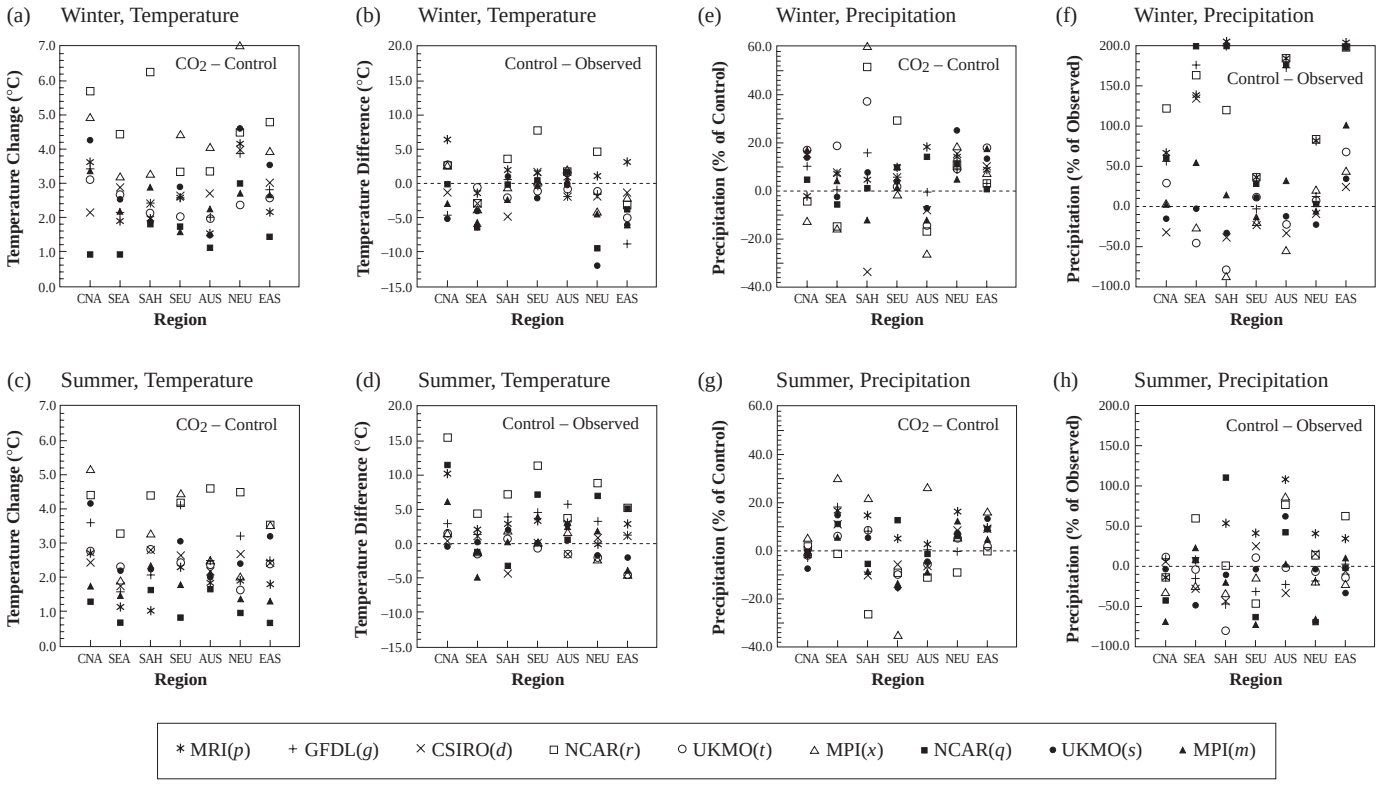

Figure B-1: Difference between averages at time of CO_2 doubling and control run averages (CO_2–Control) and difference between control run averages and observed averages (Control–Observed) as simulated by nine AOGCM runs over seven regions. Units are °C for temperature and percentage of control run, or observed, averages for precipitation. In (f) and (h), values in excess of 200% have been reported at the top end of the vertical scale. In (e), values in excess of 60% have been reported at the top end of the vertical scale. Winter averages are for December-January-February (DJF) for Northern Hemisphere regions, and June-July-August (JJA) for Australia; summer averages are for JJA for the Northern Hemisphere, and DJF for Australia. See Kittel *et al*. (1997) for further details.

change scenarios. The model runs are labeled *d*, *g*, *m*, *x*, *p*, *q*, *r*, *s*, and *t* as shown in the legend of the figure. Letter designations here refer to model descriptions in Table B-1. Note also in Table B-1 that the models employ different spatial resolutions and flux adjustments.

Scenarios produced by these transient experiments varied widely among models and from region to region, both for temperature and precipitation. Except for a few outliers, individual values of projected surface warming varied mostly in the range of ~1 to ~5°C [Figure B-1 (a,c)]—with the NCAR(*r*) and MPI(*q*) runs showing the least temperature sensitivity because, with a 1% linear increase in CO_2/year (Table B-1), CO_2 has increased only by a factor of 1.7 by the end of the 70-year simulation, compared to a doubling for the other model runs. For most regions, the inter-model range of simulated temperature increase was rather pronounced, about 3-5°C. With the exception of one or two outliers, the smallest inter-model range of simulated warming at the time of CO_2 doubling was over Australia in summer and the Sahel in winter, where the scenarios differed among models by no more than 1.3°C. It should be noted, however, that for a region such as Australia continental-scale agreement may come from canceling differences at the sub-continental scale.

The surface air temperature biases had positive and negative values both in winter and summer [Figure B-1 (b,d)]. However, biases were mostly negative in winter and positive in summer, an indication that the models tended to overestimate the seasonal temperature cycles. Most biases were in the range of -7 to 10°C, but values as large as ~15°C were found. The smallest biases were found over Australia and, with the exception of one or two models, South East Asia and Southern Europe. Over most regions, the inter-model range of temperature biases was of the order of 10°C (i.e., it was greater than the inter-model range of regional temperature increase). The surface temperature biases as well as the simulated regional warming scenarios were in the same range as those reported in IPCC (1990) for a number of equilibrium runs.

Regional precipitation biases spanned a wide range, with values as extreme as ~-90% or greater than 200% [Figure B-1 (f,h)]. The biases were generally larger in winter than in summer, and, overall, regions with the smallest biases were Southern Europe, Northern Europe, and Central North America. Regions receiving low winter precipitation (e.g., Sahel, South East Asia) tended to have large positive or negative biases, because small errors in control run values appear as large biases when reported in percentage terms.

Simulated precipitation sensitivity to doubled CO_2 was mostly in the range of -20 to 20% of the control value [Figure B-1 (e,g)]. The most salient features of simulated regional precipitation changes are summarized as follows:

- All models agreed in summer precipitation increases over East Asia and, except for one model, South East Asia—reflecting an enhancement of summer monsoonal flow (contrast this result to the experiments that include the effects of sulfate aerosols; see discussion below in relation to Figure B-2).
- All models agreed in winter precipitation increases over Northern Europe, East Asia, and, except for one model, Southern Europe. In the other cases, agreement was not found among models even on the sign of the simulated change.
- Regions with the smallest inter-model range of simulated precipitation change were Central North America, East Asia, and Northern Europe in summer and Southern Europe, Northern Europe, and East Asia in winter.
- Overall, the precipitation biases were greater than the simulated changes. A rigorous statistical analysis of the model results in Figure B-1 has not been carried out; however, it can be expected that, due to relatively high temporal and spatial variability in precipitation, temperature changes are more likely to be statistically significant than precipitation changes.

In summary, several instances occurred in which regional scenarios produced by all models agreed, at least in sign. In fact, regardless of whether flux correction was used, the range of model sensitivity was less than the range of biases (note that the scales in Figure B-1 are different for the sensitivities and the biases). However, the range of simulated scenarios of the model regional biases were still large, so that confidence in regional scenarios simulated by AOGCMs remains low. It should be pointed out that, while model agreement increases our confidence in the veracity of model responses, it does not necessarily guarantee their correctness because of possible systematic errors or deficiencies shared by all models. On the other hand, in spite of these errors, models are useful tools to study climate sensitivity (see IPCC 1996, WG I, Chapter 5). Even though models cannot exactly reproduce many details of today's climate, key processes that we know to exist in the real climate system are represented in these models (see IPCC 1996, WG I, Chapter 4). For example, the simulation of the seasonal cycle of winds, temperature, pressure, and humidity in both the horizontal and vertical provides us with a first-order qualification of the fidelity of the models' ability to capture these basic features of the Earth's climate. As another example, AOGCMs exhibit the ability to simulate essential responses of the climate system to various forcings (e.g., those involving El Niño sea surface temperature anomalies and aerosols from volcanic activity). This increases our confidence in the use of AOGCM sensitivity experiments to evaluate potential changes in important climate processes.

B.2. Simulations with Greenhouse Gas and Aerosol Forcing

Two simulations (*x*,*w*) were forced with the historical increase in equivalent CO_2, then a 1%/yr increase in equivalent CO_2. The patterns of change are qualitatively similar to those in the experiments above. In Sections 6.2.1.2 and 8.4.2.3 of the

Table B-1: *Summary of transient coupled AOGCM experiments used in this assessment. The scenario gives the rate of increase of CO_2 used; most experiments use 1%/yr, which gives a doubling of CO_2 after 70 years (IS92a gives a doubling of equivalent CO_2 after 95 years). The ratio of the transient response at the time of doubled CO_2 to the equilibrium (long-term) response to doubling CO_2 is given if known.*

Center	Expt	Reference	Flux Adjusted?	Scenario	Warming at Doubling†	Equilibrium Warming	Ratio (%)†
BMRC	*a*	Power *et al.* (1993), Colman *et al.* (1995)	No	1%/yr	1.35	2.1	63
CCC	*b*	G. Boer (pers. comm.)	Yes	1%/yr	–	3.5	
COLA	*c*	E. Schneider (pers. comm.)	No	1%/yr	2.0	–	
CSIRO	*d*	Gordon and O'Farrell (1997)	Yes	1%/yr	2.0	4.3	47
GFDL	*e*	Stouffer (pers. comm.)	Yes	0.25%/yr	*2.6*	3.7	
	f	Stouffer (pers. comm.)	Yes	0.50%/yr	*2.4*	3.7	
	g	Manabe *et al.* (1991, 1992)	Yes	1%/yr	2.2	3.7	59
	h	Stouffer (pers. comm.)	Yes	2%/yr	*1.8*	3.7	
	i	Stouffer (pers. comm.)	Yes	4%/yr	*1.5*	3.7	
	j	Stouffer (pers. comm.)	Yes	1%/yr	–	–	
GISS	*k*	Russell *et al.* (1995), Miller and Russell (1995)	No	1%/yr	1.4	–	
IAP	*l*[1]	Keming *et al.* (1994)	Yes	1%/yr	2.5	–	
MPI	*m*[2]	Cubasch *et al.* (1992, 1994b), Hasselmann *et al.* (1993), Santer *et al.* (1994)	Yes	IPCC90A	*1.3*	2.6	*50*
	n	Cubasch *et al.* (1992), Hasselmann *et al.* (1993), Santer *et al.* (1994)	Yes	IPCC90D	na	2.6	
	o		Yes	IPCC90A	*1.5*	–	
	x[3]	Hasselmann *et al.* (1995)	Yes	IPCC90A	na	2.6	
	y[4]	Hasselmann *et al.* (1995)	Yes	Aerosols	na	2.6	
MRI	*p*	Tokioka *et al.* (1995)	Yes	1%/yr	1.6	–	
NCAR	*q*	Washington and Meehl (1989)	No	1%/yr*	*2.3*	4.0	58
	r[5]	Washington and Meehl (1993, 1996), Meehl and Washington (1996)	No	1%/yr	3.8	4.6	83
UKMO	*s*	Murphy (1995a,b), Murphy and Mitchell (1995)	Yes	1%/yr	1.7	2.7	64
	t[6]	Johns *et al.* (1997), Keen (1995)	Yes	1%/yr	1.7	2.5	68
	w[7]	Johns *et al.* (1997), Tett *et al.* (1997), Mitchell *et al.* (1995b), Mitchell and Johns (1997)	Yes	1%/yr	na	2.5	
	z[8]	Johns *et al.* (1997), Tett *et al.* (1997), Mitchell *et al.* (1995b), Mitchell and Johns (1997)	Yes	Aerosols	na	2.5	

na = not available

†Numbers in italics indicate simulations with other than a 1%/yr increase in CO_2.

*1%/yr of current CO_2 concentrations.

[1]Polar deep ocean quantities constrained.

[2]Three additional 50-year runs, each from different initial conditions.

[3]CO_2 from IPCC scenario 90A after greenhouse gas forcing from 1880 to 1990.

[4]As (1) with a representation of aerosol forcing, with increases after 1990 based on IS92a.

[5]Equilibrium model excluded sea ice dynamics. Coupled model has warmer than observed tropical sea surface temperatures and a vigorous ice albedo feedback (Washington and Meehl, 1996) contributing to the high sensitivity.

[6]Average of three experiments from different initial conditions.

[7]CO_2 increased by 1%/yr from 1990. Observed greenhouse gas forcing used from 1860 to 1990.

[8]As (7) with a representation of aerosol forcing, with increases of aerosol and greenhouse gases after 1990 based on IS92a.

Working Group I contribution to IPCC (1996), we saw that the inclusion of the direct sulfate aerosol forcing can improve the simulation of the patterns of temperature change over the last few decades. Here we consider the effect of combined greenhouse gas and direct sulfate aerosol forcing derived from IS92a on simulated patterns of temperature change to 2050 and beyond (*y*,*z*). Figure B-2 shows area averages of summer and winter surface temperature, precipitation, and soil moisture from two models—one set with CO_2 increase only, the other with CO_2 increase and the direct effects of sulfate aerosols. The areas considered include five from Figure B-1 (i.e., Central North America, South East Asia, Sahel, Southern Europe, and Australia).

Increasing CO_2 alone leads to positive radiative forcing everywhere, with the largest radiative heating in regions of clear skies and high temperatures (experiment *w* shown in Figure 6.7a of IPCC 1996, WG I). The surface temperature warms everywhere except in the northern North Atlantic (Figure 6.7b of IPCC 1996, WG I). In transient simulations to 2050, the inclusion of aerosols based on IS92a (*y*,*z*) reduces the global mean radiative forcing, and leads to negative radiative forcing over southern Asia. This leads to a muted warming or even small regions of cooling (*y*) in mid-latitudes. In (*z*), China continues to warm, albeit at a very reduced rate, even though the local net radiative forcing becomes increasingly negative (Figure 6.7c in IPCC 1996, WG I). The rate of warming over North America and western Europe, where the aerosol forcing weakens, remains below that in the simulation with greenhouse gases only (*w*). The cooling due to aerosols is amplified by sea ice feedbacks in the Arctic (Figure 6.7f in IPCC 1996, WG I).

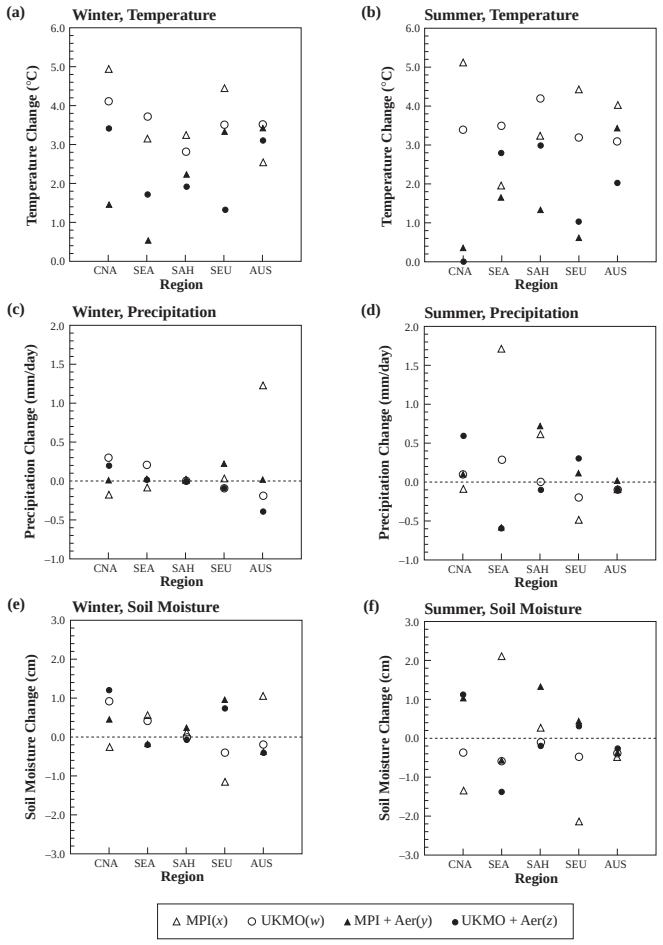

Figure B-2: Simulated regional changes from 1880–1889 to 2040–2049 (experiments *x*, *y*) or from pre-industrial to 2030–2050 (experiments *w*, *z*). Experiments *x* and *w* include greenhouse gas forcing only, whereas *y* and *z* also include direct sulfate aerosol effects (see Table B-1): (a) Temperature (December to February); (b) Temperature (June to August); (c) Precipitation (December to February); (d) Precipitation (June to August); (e) Soil Moisture (December to February); and (f) Soil Moisture (June to August).

In assessing these results, one should bear in mind the possible exaggeration of the sulfate aerosol concentrations under this scenario, the uncertainties in representing the radiative effects of sulfate aerosols, and neglect of other factors including the indirect effect of sulfates. Nevertheless, these experiments suggest that the direct effect of sulfate aerosols could have strong influence on future temperature changes, particularly in northern mid-latitudes.

B.3. Seasonal Changes in Temperature, Precipitation, and Soil Moisture

IPCC (1990) reported some broad scale changes that were evident in most of the equilibrium $2xCO_2$ experiments that were then available. The detailed regional changes differed from model to model. In the transient experiments reported in IPCC (1992), it was found that the large-scale patterns of response at the time of doubling CO_2 were similar to the corresponding equilibrium experiments (IPCC, 1990), except that there was a smaller warming in the vicinity of the northern North Atlantic and the Southern Ocean in transient experiments. Here we summarize the main features in the seasonal (December to February and June to August) patterns of change in temperature, precipitation, and soil moisture in those experiments with a 1%/yr increase in CO_2 for which data were available. The changes are assessed at the time data of CO_2 doubling (after 70 years). In experiments *w*-*z*, we also contrast the continental-scale response under the IS92a scenario with and without aerosol forcing at around 2040.

B.3.1. Temperature

With increases in CO_2, all models produce a maximum annual mean warming in high northern latitudes (Figures 6.6 and 6.7b of IPCC 1996, WG I). The warming is largest in late autumn and winter, largely due to sea ice forming later in the warmer climate. In summer, the warming is small; if the sea ice is removed with increased CO_2, then the thermal inertia of the mixed-layer prevents substantial warming during the short summer season, otherwise melting sea ice is present in both control and anomaly simulations, and there is no change in

surface temperature (see Ingram *et al*., 1989). The details of these changes are sensitive to parameterization of sea ice and, in particular, the specification of sea ice albedo (e.g., Meehl and Washington, 1995). In one simulation (*k*), there is a marked cooling over the northeastern Atlantic throughout the year, which leads to a cooling over part of northwest Europe in winter. There is little seasonal variation of the warming in low latitudes or over the southern circumpolar ocean.

When aerosol effects are included (*y*,*z* cf. *x*,*w* respectively), the maximum winter warming in high northern latitudes is less extensive. In mid-latitudes, there are some regions of cooling (e.g., over China), and the mean warming in the tropics is greater than in mid-latitudes. In northern summer, there are again regions of cooling in mid-latitudes and the greatest warming now occurs over Antarctica. Again, including the direct forcing by sulfate aerosols has a strong effect on simulated regional temperature changes, though the reader should bear in mind the limitations of these experiments as noted earlier.

B.3.2. Precipitation

On increasing CO_2, all models produce an increase in global mean precipitation. Precipitation increases in high latitudes in winter (except in *k* around the Norwegian Sea where there is cooling and a reduction in precipitation), and in most cases the increases extend well into mid-latitudes (e.g., Figure 6.11a in IPCC 1996, WG I). The warming of the atmosphere leads to higher atmospheric water vapor content and enhanced poleward water vapor transport into the northern high latitudes—hence enhanced water vapor convergence and precipitation (e.g., Manabe and Wetherald, 1975). In the tropics, the patterns of change vary from model to model, with shifts or changes in intensity of the main rainfall maxima. However, many produce more rainfall over India and/or southeast Asia as seen in Figure B-1. This is consistent with an increase in atmospheric water vapor concentration leading to enhanced low level moisture convergence associated with the strong mass convergence into the monsoon surface pressure low. All models considered apart from *p* and *q* produce a general reduction in precipitation over southern Europe. In general, changes in the dry subtropics are small.

With the inclusion of aerosol forcing (*y*,*z*), there is only a small increase in global mean precipitation. The patterns of change in precipitation in northern winter are broadly similar to that in a parallel simulation with greenhouse gases only (*x*,*w* respectively), but less intense. In northern summer, there is a net reduction in precipitation over the Asian monsoon region (Figure B-2), because the aerosol cooling reduces the land-sea contrast and the strength of the monsoon flow. This is in contrast to the models run with CO_2 increase only that showed increases of monsoon precipitation (Figure B-1). Precipitation increases on average over southern Europe (it decreases when aerosol effects are omitted) and over North America, where changes were small with increases in greenhouse gases only.

There is now mounting evidence to suggest that a warmer climate will be one in which the hydrological cycle will in general be more intense (IPCC, 1992), leading to more heavy rain events (*ibid*, pp. 119). It should be noted, however, that as the GCM grid sizes are much larger than convective elements in the atmosphere, daily precipitation is poorly reproduced by GCMs.

B.3.3. Soil Moisture

Soil moisture may be a more relevant quantity for assessing the impacts of changes in the hydrological cycle on vegetation than precipitation since it incorporates the integrated effects of changes in precipitation, evaporation, and runoff throughout the year. However, simulated changes in soil moisture should be viewed with caution because of the simplicity of the land-surface parameterization schemes in current models (e.g., experiments *a*,*e*-*i*,*m*,*n*,*p*,*q*, and *r* use an unmodified "bucket" formulation; see Section 5.3.2 of IPCC 1996, WG I).

Most models produce a general increase in soil moisture in the mean in high northern latitudes in winter, though in some (*a*,*k*) there are also substantial areas of reduction. The increases are due mainly to the increased precipitation discussed above, and the increased reaction of precipitation falling as rain in the warmer climate. At the low winter temperatures, the absolute change in potential evaporation is small, as expected from the Clausius-Clapyeron relation, so evaporation increases little even though temperature increases are a maximum in winter. Hence, the increase in soil moisture in high altitudes in winter is consistent with physical reasoning and the broad scale changes are unlikely to be model-dependent. However, it should be noted that in general the models considered here do not represent the effects of freezing on groundwater.

Most models produce a drier surface in summer in northern mid-latitudes. This occurs consistently over southern Europe (except *q*, which produces an excessively dry surface in winter in its control climate) and North America (except *d*,*k*, and *q*). The main factor in the drying is enhanced evaporation in summer (see Wetherald and Manabe, 1995): The absolute rate of increase in potential evaporation increases exponentially with temperature if other factors (wind, stability, and relative humidity) are unchanged.

As noted in the IPCC (1990), the following factors appear to contribute to summer drying:

- The soil in the control simulation is close to saturation in late winter or spring; this ensures that much of the extra precipitation in winter is not stored in the soil but lost as runoff.
- There is a substantial seasonal variation in soil moisture in the simulation of present climate; some of the simpler models may exaggerate the seasonal cycle of soil moisture (see Chapter 5 of IPCC 1996, WG I) leading to an exaggerated response in the warmer climate.

- In higher latitudes, earlier snowmelt leading to enhanced solar absorption and evaporation may contribute.
- Changes in soil moisture may be amplified by cloud feedbacks in regions where evaporation is being limited by low soil moisture values (e.g., Wetherald and Manabe, 1995).
- The drying is more pronounced in regions where precipitation is reduced in summer.

Given the varying response of different land-surface schemes to the same prescribed forcing (IPCC 1996, WG I, Chapter 5), the consistency from model to model of reductions over southern Europe in summer might be regarded as surprising. All models submitted (except *p*,*q*) produced a reduction in summer precipitation over southern Europe: Here changes in circulation and precipitation may be more important in determining soil moisture changes than the details of the land-surface scheme. Reductions over North America are less consistent, and there is a still wider model-to-model variation in the response over northern Europe and northern Asia.

With aerosol forcing included (*y*,*z*), the patterns of soil moisture change in northern winter are similar but weaker than with greenhouse gas forcing only (*x*,*w*). However, soil moisture increases over North America and southern Europe in summer when aerosol effects are included (*y*,*z*), presumably because of the reduced warming and its effect on evaporation, and because of increases in precipitation. The changes in the hydrological cycle are likely to be sensitive to the distribution of aerosol forcing and the coupled model used. However, it is clear that aerosol effects have a strong influence on simulated regional climate change.

B.4. Simulations using Statistical Downscaling and Regional Climate Modeling Systems

Although computing power has substantially increased during the last few years, the horizontal resolution of present coupled GCMs is still too coarse to capture the effects of local and regional forcings in areas of complex surface physiography and to provide information suitable for many impact assessment studies. Since IPCC (1992), significant progress has been achieved in the development and testing of statistical downscaling and regional modeling techniques for the generation of high-resolution regional climate information from coarse-resolution GCM simulations.

B.4.1. Statistical Downscaling

Statistical downscaling is a two-step process basically consisting of i) development of statistical relationships between local climate variables (e.g., surface air temperature and precipitation) and large-scale predictors, and ii) application of such relationships to the output of GCM experiments to simulate local climate characteristics. A range of statistical downscaling models have been developed (IPCC 1996, WG I), mostly for U.S., European, and Japanese locations where better data for model calibration are available. The main progress achieved in the last few years has been the extension of many downscaling models from monthly and seasonal to daily time scales, which allows the production of data more suitable for a broader set of impact assessment models (e.g., agriculture or hydrologic models).

When optimally calibrated, statistical downscaling models have been quite successful in reproducing different statistics of local surface climatology (IPCC 1996, WG I). Limited applications of statistical downscaling models to the generation of climate change scenarios has occurred showing that in complex physiographic settings local temperature and precipitation change scenarios generated using downscaling methods were significantly different from, and had a finer spatial scale structure than, those directly interpolated from the driving GCMs (IPCC 1996, WG I).

B.4.2. Regional Modeling

The (one-way) nested modeling technique has been increasingly applied to climate change studies in the last few years. This technique consists of using output from GCM simulations to provide initial and driving lateral meteorological boundary conditions for high-resolution Regional Climate Model (RegCM) simulations, with no feedback from the RegCM to the driving GCM. Hence, a regional increase in resolution can be attained through the use of nested RegCMs to account for sub-GCM grid-scale forcings. The most relevant advance in nested regional climate modeling activities was the production of continuous RegCM multi-year climate simulations. Previous regional climate change scenarios were mostly produced using samples of month-long simulations (IPCC 1996, WG I). The primary improvement represented by continuous long-term simulations consists of equilibration of model climate with surface hydrology and simulation of the full seasonal cycle for use in impact models. In addition, the capability of producing long-term runs facilitates the coupling of RegCMs to other regional process models, such as lake models, dynamical sea ice models, and possibly regional ocean (or coastal) and ecosystem models.

Continuous month- or season-long to multi-year experiments for present-day conditions with RegCMs driven either by analyses of observations or by GCMs were generated for regions in North America, Asia, Europe, Australia, and Africa. Equilibrium regional climate change scenarios due to doubled CO_2 concentration were produced for the continental U.S., Tasmania, Eastern Asia, and Europe. None of these experiments included the effects of atmospheric aerosols.

In the experiments mentioned above, the model horizontal grid point spacing varied in the range of 15 to 125 km and the length of runs from 1 month to 10 years. The main results of the validation and present-day climate experiments with RegCMs can be summarized in the following points:

- When driven by analyses of observations, RegCMs simulated realistic structure and evolution of synoptic

events. Averaged over regions on the order of 10^4–10^6 km^2 in size, temperature biases were mostly in the range of a few tenths of °C to a few °C, and precipitation biases were mostly in the range of 10–40% of observed values. The biases generally increased as the size of the region decreased.

- The RegCM performance was critically affected by the quality of the driving large-scale fields, and tended to deteriorate when the models were driven by GCM output, mostly because of the poorer quality of the driving large-scale data compared to the analysis data (e.g., position and intensity of storm tracks).
- Compared to the driving GCMs, RegCMs generally produced more realistic regional detail of surface climate as forced by topography, large lake systems, or narrow land masses. However, the validation experiments also showed that RegCMs can both improve and degrade aspects of regional climate compared to the driving GCM runs, especially when regionally averaged.
- Overall, the models performed better at mid-latitudes than in tropical regions.
- The RegCM performance improved as the resolution of the driving GCM increased, mostly because the GCM simulation of large-scale circulation patterns improved with increasing resolution.
- Seasonal as well as diurnal temperature ranges were simulated reasonably well.
- An important problem in the validation of RegCMs has been the lack of adequately dense observational data, since RegCMs can capture fine structure of climate patterns. This problem is especially relevant in mountainous areas, where only a relatively small number of high-elevation stations are often available.

When applied to the production of climate change scenarios, nested model experiments showed the following (IPCC 1996, WG I):

- For temperature, the differences between RegCM- and GCM-simulated region-averaged change scenarios were in the range of 0.1 to 1.4°C. For precipitation, the differences between RegCM and GCM scenarios were more pronounced than for temperature, in some instances by one order of magnitude or even in sign. These differences between RegCM- and GCM-produced regional scenarios are due to the combined contributions of the different resolution of surface forcing (e.g., topography, lakes, coastlines) and atmospheric circulations, and in some instances the different behavior of model parameterizations designed for the fine- and coarse-resolution models. In summer, differences between RegCM and GCM results were generally more marked than in winter due to the greater importance of local processes.
- While the simulated temperature changes obtained with nested models were generally larger than the corresponding biases, the precipitation changes were generally of the same order of, or smaller than, the precipitation biases.

Finally, of relevance for the simulation of regional climate change is the development of a variable-resolution global model technique, whereby the model resolution gradually increases over the region of interest.

B.5. Conclusions

Analysis of surface air temperature and precipitation results from regional climate change experiments carried out with AOGCMs indicates that the biases in present-day simulations of regional climate change and the inter-model variability in the simulated regional changes are still too large to yield a high level of confidence in simulated change scenarios. The limited number of experiments available with statistical downscaling techniques and nested regional models has shown that complex topographical features, large lake systems, and narrow land masses not resolved at the resolution of current GCMs significantly affect the simulated regional and local change scenarios, both for precipitation and (to a lesser extent) temperature (IPCC 1996, WG I). This adds a further degree of uncertainty in the use of GCM-produced scenarios for impact assessments. In addition, most climate change experiments have not accounted for human-induced landscape changes and only recently has the effect of aerosols been investigated. Both these factors can further affect projections of regional climate change.

Compared to the global-scale changes due to doubled CO_2 concentration, the changes at 10^4–10^6 km^2 scale derived from transient AOGCM runs are greater. Considering all models, at the 10^4–10^6 km^2 scale, temperature changes due to CO_2 doubling varied between 0.6 and 7°C and precipitation changes varied between -35 and 50% of control run values, with a marked inter-regional variability. Thus, the inherent predictability of climate diminishes with reduction in geographical scale. The greatest model agreement in the simulated precipitation change scenarios was found over the South East Asia (about -1 to 30%), Northern Europe (about -9 to 16%), Central North America (about -7 to 5%), and East Asia (about 0.1 to 16%) regions in summer, and Southern Europe (about -2 to 29%), Northern Europe (about 5 to 25%), and East Asia (about 0.5 to 18%) in winter. For temperature, the greatest model agreement in simulated warming occurred over Australia in summer (about 1.65 to 2.5°C, when excluding one outlier) and the Sahel in winter (about 1.8 to 3.15°C, when excluding one outlier). Regardless of whether flux correction was used, the range of model sensitivities was less than the range of biases, which suggests that models produce regional sensitivities that are more similar to each other than their biases.

The latest regional model experiments indicate that high-resolution information, on the order of a few 10s of km or less, may be necessary to achieve high accuracy in regional and local change scenarios in areas of complex physiography. In the last few years, substantial progress has been achieved in the development of tools for enhancing GCM information. Statistical methods were extended from the monthly/seasonal to the daily time scale, and nested model experiments were

extended to the multi-year time scale. Also, variable- and high-resolution global models can be used to study possible feedbacks of mesoscale forcings on general circulation.

Regional modeling techniques, however, rely critically on the GCM performance in simulating large-scale circulation patterns at the regional scale, because they are a primary input to both empirical and physically based regional models. Although the regional performance of coarse-resolution GCMs is still somewhat poor, there are indications that features such as positioning of storm track and jet stream core are better simulated as the model resolution increases. The latest nested GCM/RegCM and variable-resolution model experiments, which employed relatively high-resolution GCMs and were run for long simulation times (up to 10 years) show an improved level of accuracy. Therefore, as a new generation of higher resolution GCM simulations become available, it is expected that the quality of simulations with regional and local downscaling models will also rapidly improve. In addition, the movement towards coupling regional atmospheric models with appropriately scaled ecological, hydrological, and mesoscale ocean models will not only improve the simulation of climatic sensitivity, but also provide assessments of the joint response of the land surface, atmosphere, and/or coastal systems to altered forcings.

References

Colman, R.A., S.B. Power, B.J. MacAvaney and R.R. Dahni, 1995: A non-flux-corrected transient CO_2 experiment using the BMRC coupled atmosphere/ocean GCM. *Geophysical Research Letters*, **22**, 3047-3050.

Cubasch, U., K. Hasselmann, H. Höck, E. Maier Reimer, U. Mikolajewicz, B.D. Santer, and R. Sausen, 1992: Time-dependent greenhouse warming computations with a coupled ocean-atmosphere model. *Climate Dynamics*, **8**, 55-69.

Cubasch, U., G. Meehl, and Z.C. Zhao, 1994a: *IPCC WG I Initiative on Evaluation of Regional Climate Change*. Summary Report, 12 pp.

Cubasch, U., B.D. Santer, A. Hellach, G. Hegerl, H. Höck, E. Maier-Reimer, U. Mikolajewicz and A. Stössl, 1994b: Monte Carlo climate change forecasts with a global coupled ocean-atmosphere model. *Climate Dynamics*, **10**, 1-20.

Gordon, H.B. and S.P. O'Farrell, 1997: Transient climate change in the CSIRO coupled model with dynamical sea-ice. *Monthly Weather Review*, **125**, 875-907.

Hasselmann, K, R. Sausen, E. Maier-Reimer and R. Voss, 1993: On the cold start problem in transient simulations with coupled ocean-atmosphere models. *Climate Dynamics*, **9**, 53-61.

Hasselmann K., L. Bengtsson, U. Cubasch, G.C. Hegerl, H. Rodhe, E. Roeckner, H. von Storch, R. Voss, and J. Waszkewitz, 1995: Detection of anthropogenic climate change using a fingerprint method. In: *Proceedings of "Modern Dynamical Meteorology," Symposium in honor of Aksel Wiin-Nielsen, 1995* [P. Ditlevsen (ed.)]. ECMWF Press.

Ingram, W.J., C.A. Wilson, and J.F.B. Mitchell, 1989: Modeling climate change: An assessment of sea-ice and surface albedo feedbacks. *Journal of Geophysical Research*, **94**, 8609-8622.

IPCC, 1990: *Climate Change: The IPCC Scientific Assessment* [Houghton, J.T., G.J. Jenkins, and J.J. Ephraums (eds.)]. Cambridge University Press, Cambridge and New York, 365 pp.

IPCC, 1992. *Climate Change 1992: The Supplementary Report to the IPCC Scientific Assessment.* Report of the IPCC Scientific Assessment Working Group [Houghton, J.T., B.T. Callander, and S.K. Varney (eds.)]. Cambridge University Press, Cambridge and New York, 200 pp.

IPCC, 1996: *Climate Change 1995: The Science of Climate Change.* Contribution of Working Group I to the Second Assessment Report of the Intergovernmental Panel on Climate Change [Houghton, J.J., L.G. Meiro Filho, B.A. Callander, N. Harris, A. Kattenberg and K.Maskell (eds.)]. Cambridge University Press, Cambridge and New York, 572 pp.

Johns, T.C., R.E. Carnell, J.F. Crossley, J.M. Gregory, J.F.B. Mitchell, C.A. Senior, S.F.B. Tett, and R.A. Wood, 1997: The second Hadley Centre coupled ocean-atmosphere GCM: Model description, spinup and validation. *Climate Dynamics*, **13**, 103-134.

Keen, A.B., 1995: Investigating the effects of initial conditions on the response of the Hadley Centre coupled model. *Hadley Centre Internal Note no. 71*.

Keming, C., J. Xiangze, L. Wuyin, Y. Yongquiang, G. Yufu, and Z. Xuehong, 1994: Lecture in International Symposium on Global Change in Asia and the Pacific Region (GCAP). 8-10 Aug, 1994, Beijing.

Kittel, T.G.F., N.A. Rosenbloom, T.H. Painter, D.E. Schimel, and VEMAP modeling participants, 1995: The VEMAP integrated database for modeling United States ecosystem/vegetation sensitivity to climate change. *Journal of Biogeography*, **22**, 857-862.

Kittel, T.G.F., F. Giorgi and G.A. Meehl, 1997: Intercomparison of regional biases and doubled CO_2 sensitivity of coupled atmosphere-ocean general circulation model climate experiments. *Climate Dynamics* (in press).

Li, X., Z. Zongci, W. Shaowu, and D. Yohui, 1994: Evaluation of regional climate change simulation: A case study. *Proceedings of the IPCC Special Workshop on Article 2 of the United Nations Framework Convention on Climate Change*. Fortaleza, Brazil, 17-21 October 1994.

Manabe, S. and R.T. Wetherald, 1975: The effects of doubling the CO_2 concentration on the climate of a general circulation model. *Journal of Atmospheric Sciences*, **32**, 3-15.

Manabe, S., R.J. Stouffer, M.J. Spelman, and K. Bryan, 1991: Transient responses of a coupled-ocean atmosphere model to gradual changes of atmospheric CO_2. Part I: Annual mean response. *Journal of Climate*, **4**, 785-818.

Manabe, S., M.J. Spelman, and R.J. Stouffer, 1992: Transient responses of a coupled ocean-atmosphere model to gradual changes of atmospheric CO_2. Part II: Seasonal response. *Journal of Climate*, **5**, 105-126.

Mearns, L.O., F. Giorgi, L. McDaniel, and C. Shields, 1995a: Analysis of daily variability of precipitation in a nested regional climate model: Comparison with observations and doubled CO_2 results. *Global and Planetary Change*, **10**, 55-78.

Mearns, L.O., F. Giorgi, L. McDaniel, and C. Shields, 1995b: Analysis of variability and diurnal range of daily temperature in a nested regional climate model: Comparison with observations and doubled CO_2 results. *Climate Dynamics*, **11**, 193-209.

Meehl, G.A. and W.M. Washington, 1995: Cloud albedo feedback and the super greenhouse effect in a global coupled GCM. *Climate Dynamics*, **11**, 399-411.

Meehl, G.A. and W.M. Washington, 1996: El Niño-like climate change in a model with increased atmospheric CO_2 concentrations. *Nature*, **382**, 56-60.

Miller, J.R. and G.L. Russell,1995: Climate change and the Arctic hydrologic cycle as calculated by a global coupled atmosphere-ocean model. *Annual Glaciology*, **21**, 91-95.

Mitchell, J.F.B. and T.J. Johns, 1997: On modification of global warming by sulfate aerosols. *Journal of Climate*, **10**, 245-267.

Mitchell, J.F.B., R.A. Davis, W.J. Ingram, and C.A. Senior, 1995b: On surface temperature, greenhouse gases and aerosols: models and observations. *Journal of Climate*, **10**, 2364-2386.

Murphy, J.M., 1995a: Transient response of the Hadley Centre coupled model to increasing carbon dioxide. Part I – Control climate and flux adjustment. *Journal of Climate*, **8**, 36-56.

Murphy, J.M., 1995b: Transient response of the Hadley Centre coupled model to increasing carbon dioxide. Part III – Analysis of global-mean response using simple models. *Journal of Climate*, **8**, 496-514.

Murphy, J.M. and J.F.B. Mitchell, 1995: Transient response of the Hadley Centre coupled model to increasing carbon dioxide. Part II – Temporal and spatial evolution of patterns. *Journal of Climate*, **8**, 57-80.

Power, S., R. Colman, B. McAvaney, R. Dahni, A. Moore, and N. Smith, 1993: The BMRC coupled atmosphere/ocean/sea ice model. *The BMRC Research Report No 37.*

Raisanen, J., 1995: A comparison of the results of seven GCM experiments in Northern Europe. *Geophysica*, **30(1-2)**, 3-30.

Russell, G.L., J.R. Miller, and D. Rind, 1995: A coupled atmosphere-ocean model for transient climate change studies. *Atmosphere-Ocean*, **33**, 4.

Santer, B.D., W. Bruggemann, U. Cubasch, K. Hasselmann, E. Maier-Reimer, and U. Mikolajewicz, 1994: Signal-to-noise analysis of time-dependent greenhouse warming experiments. Part 1: Pattern analysis. *Climate Dynamics*, **9**, 267-285.

Tett, S.F.B., T.C. Johns, and J.F.B. Mitchell, 1997: Global and regional variability in a coupled AOGCM. *Climate Dynamics*, **13**, 303-323.

Tokioka, T., A. Noda, A. Kitoh, Y. Nikaidou, S. Nakagawa, T. Motoi, S. Yukimoto, and K. Takata, 1995: A transient CO_2 experiment with the MRI CGCM. *Journal of the Meteorological Society of Japan*, **74(4)**, 817-826.

Washington, W.M. and G.A. Meehl, 1989: Climate sensitivity due to increased CO_2: Experiments with a coupled atmosphere and ocean general circulation model. *Climate Dynamics*, **4**, 1-38.

Washington, W.M. and G.A. Meehl, 1993: Greenhouse sensitivity experiments with penetrative cumulus convection and tropical cirrus albedo effects. *Climate Dynamics*, **8**, 211-223.

Washington, W.M. and G.A. Meehl, 1996: High-latitude climate change in a global coupled ocean-atmosphere-sea ice model with increased atmospheric CO_2. *Journal of Geophysical Research*, **101**, 12795-12801.

Wetherald, R.T. and S. Manabe, 1995: The mechanisms of summer dryness induced by greenhouse warming. *Journal of Climate*, **8**, 3096-3108.

Whetton, P.H., P.J. Rayner, A.B. Pittock, and M.R. Haylock, 1994: An assessment of possible climate change in the Australian region based on an intercomparison of general circulation modeling results. *Journal of Climate*, **7**, 441-463.

Whetton, P., M. England, S. O'Farrell, I. Waterson, and B. Pittock, 1996: Global comparison of the regional rainfall results of enhanced greenhouse coupled and mixed layer ocean experiments: Implications for climate change scenario development. *Climatic Change*, **33**, 497-519.